Low-Temperature Low-Field Phases of the Pyrochlore Quantum Magnet Tb_{2}Ti_{2}O_{7}

L. Yin, J. S. Xia, Y. Takano, N. S. Sullivan, Q. J. Li, and X. F. Sun

Phys. Rev. Lett. **110**, 137201 — Published 25 March 2013

DOI: 10.1103/PhysRevLett.110.137201

Low-Temperature Low-Field Phases of the Pyrochlore Quantum Magnet $Tb_2Ti_2O_7$

L. Yin,[1,*] J. S. Xia,[1] Y. Takano,[1] N. S. Sullivan,[1] Q. J. Li,[2] and X. F. Sun[2,†]

[1] *National High Magnetic Field Laboratory and Department of Physics, University of Florida, Gainesville, FL 32611, USA*

[2] *Hefei National Laboratory for Physical Sciences at Microscale, University of Science and Technology of China, Hefei, Anhui 230026, People's Republic of China*

By means of ac magnetic-susceptibility measurements, we find evidence for a new magnetic phase of $Tb_2Ti_2O_7$ below about 140 mK in zero magnetic field. In magnetic fields parallel to [111], this phase is characterized by frequency- and amplitude-dependent susceptibility and extremely slow spin dynamics. In the zero-temperature limit, it extends to about 67 mT (the internal field $H_{int} \simeq 52$ mT), at which it makes transition to another phase. The field dependence of the susceptibility of this second phase, which extends to about 0.60 T ($H_{int} \simeq 0.54$ T) in the zero-temperature limit, indicates the presence of a weak magnetization plateau below about 50 mK, as has been predicted by a single-tetrahedron four-spin model, suggesting that the second phase is a quantum kagome ice.

PACS numbers: 75.30.Kz, 75.40.Cx, 75.40.Gb, 75.50.Lk

In rare-earth-titanate pyrochlores, $R_2Ti_2O_7$, trivalent rare-earth ions R^{3+} with eightfold oxygen coordination form a three-dimensional lattice of corner-sharing tetrahedra. Alternatively, these magnetic oxides can be viewed as kagome layers of rare-earth spins coupled via interspacing triangular lattices of rare-earth spins, stacked along the [111] direction. In either view, the geometry leads to frustrated nearest-neighbor exchange interactions, whose interplay with an anisotropy dictated by a local <111> direction, dipole-dipole interaction, and quantum fluctuations in some cases, result in various exotic magnetic ground states [1]. $Dy_2Ti_2O_7$ and $Ho_2Ti_2O_7$ are spin ices of classical Ising spins [2–5]. By contrast, $Gd_2Ti_2O_7$ and $Er_2Ti_2O_7$ undergo magnetic transitions at temperatures of the order of 1 K, but their ground states are unconventional, with fluctuations persisting down to 20 mK [6, 7]. The most enigmatic are $Tb_2Ti_2O_7$ [8–17] and $Yb_2Ti_2O_7$ [18–21], which are under intense investigation.

In $Tb_2Ti_2O_7$, no long-range order has been found by muon-spin relaxation (μSR) down to 70 mK and by neutron scattering to 50 mK [8, 10], two orders of magnitude lower than the absolute value of the crystal-field-subtracted Curie-Weiss temperature, about -13 K or -7.0 K [22, 23], raising the possibility that this magnet is a long-sought three-dimensional quantum spin liquid. Indeed, inelastic neutron scattering suggests a crossover from a thermally disordered paramagnet to a spin liquid at about 0.4 K [13]. But a sharp peak in specific heat, suggestive of long-range ordering, has been observed at 0.37 K by a semi-adiabatic method [11], although no peak has been detected by a relaxation method in a different sample [12]. On the other hand, a muon-spin-rotation (μSR) frequency shift in low magnetic fields, 20 mT and 60 mT, applied along the [110] direction suggests a transition at a lower temperature of about 150 mK, a transition which has not been identified [12]. The static magnetic susceptibility of a zero-field-cooled polycrystalline sample in a 1 mT field shows history dependence suggestive of spin-glass behavior below about 100 mK, with an anomaly at about 70 mK interpreted as the spin-glass transition from the high-temperature phase [9].

Numerical diagonalization of a single-tetrahedron four-spin model predicts [24, 25] that the zero-field ground state of $Tb_2Ti_2O_7$ is a quantum spin liquid, dubbed a quantum spin ice [24, 26], which—with low increasing field along the [111] direction—gradually turns into a partially polarized state akin to the kagome-ice state [27, 28] of classical spin-ice magnets. At higher fields, $H \geq 82$ mT, it evolves into a "three-in one-out" state, with three spins pointing into and one pointing out of every tetrahedron. The partially polarized state, the quantum kagome ice, will manifest itself as a magnetization plateau spanning from 18 mT to 82 mT, a feature detectable at and below 20 mK.

Motivated by this prediction, we have made systematic measurements of the ac magnetic susceptibility of $Tb_2Ti_2O_7$ in zero magnetic field and fields up to 1.5 T, applied along [111]. We find evidence for a new phase bounded in zero field at 140 mK and, in the limit of zero temperature, at about 67 mT. In this phase, $Tb_2Ti_2O_7$ exhibits frequency- and amplitude-dependent susceptibility and extremely slow spin dynamics, which is observed as the temperature is swept or the ac frequency is changed stepwise. At 16 mK, the susceptibility indicates the presence of a weak magnetization plateau, adjacent to the low-field phase and extending to 0.59 T—in qualitative, but not quantitative, agreement with the prediction.

The method of sample fabrication is similar to that of Ref. [29]. A single crystal of $Tb_2Ti_2O_7$ was grown by the floating-zone technique at a rate of 2.5 mm/hour in a 0.3 MPa oxygen atmosphere. The sample was approximately a square cuboid, 4 mm × 2.4 mm × 2.4 mm, cut from the crystal with the long edges parallel to [111]. The setup for ac susceptibility measurements has been

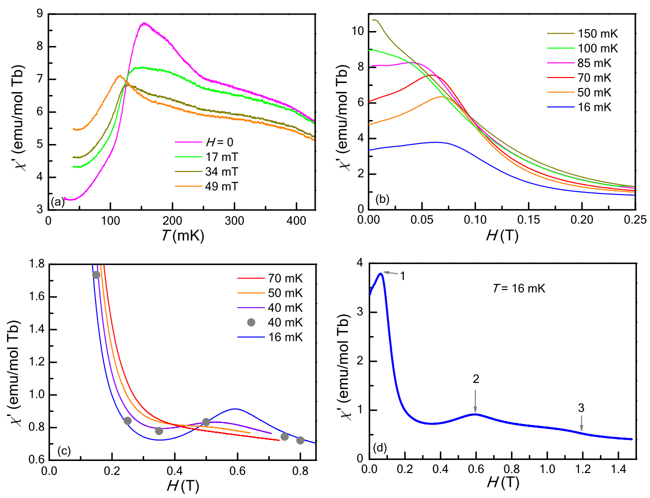

FIG. 1. (color online). (a) χ' as a function of temperature at various magnetic fields up to 49 mT, measured during upward temperature sweeps at 0.6 mK/min. The frequency and amplitude of the ac field were 0.21 Hz and 0.94 mT. (b) χ' as a function of magnetic field up to 0.25 T at various temperatures. At and above 85 mK, the frequency and amplitude of the ac field and the field-sweep rate were 87.6 Hz, 0.94 mT, and 4.2 mT/min. For lower temperatures, they were reduced to 9.6 Hz, 0.20 mT, and 0.625 mT/min. (With the ac-field amplitude of 0.94 mT, the 100 mK and 85 mK data were taken in a slightly nonlinear regime, at least at $H = 0$. See the Supplemental Material [33].) (c) The data at and below 70 mK over a wider field range. Lines are field-sweep data. Circles are equilibrium data at 40 mK. (d) The 16 mK data up to 1.5 T, arrows indicating anomalies discussed in the text. See the Supplemental Material [33] for χ''.

described elsewhere [30–32]. The ac field was applied along the [111] direction, as was the dc field. The ac frequencies ranged from 0.21 Hz to 87.6 Hz, and the ac-field amplitude, H_{ac}, was 0.20 mT or 0.94 mT. In addition, frequencies up to 389.6 Hz were used to measure spin relaxation, and amplitudes ranging from 0.048 mT to 1.2 mT were used in a nonlinearity study described in the Supplemental Material [33]. Immersing the sample in liquid ^{3}He, which in turn was cooled by a dilution refrigerator, allowed us to make reliable measurements to at least 16 mK, lower than in any previous experiment on $Tb_2Ti_2O_7$.

Shown in Fig. 1 are the real part, χ', of the susceptibility as functions of temperature and magnetic field, for temperatures up to 430 mK and fields up to 1.5 T [34]. Because of the extremely slow relaxation of the spins, a subject discussed later in detail, the temperature was raised very slowly upward at a rate of 0.6 mK/min in temperature sweeps. For field sweeps, the sweep rate at temperatures down to 86 mK was 4.2 mT/min, which was reduced to 0.625 mT/min at lower temperatures in order to ensure a nearly equilibrium condition (see the Supplemental Material [33]). As a result of the extremely slow relaxation, most of our data, even those at 0.21 Hz, were taken in the adiabatic limit, not the isothermal limit.

At zero field, a peak appears in χ' at 154 mK. When a small magnetic field, up to 49 mT, is applied along [111], the peak becomes smaller and moves to lower temperatures, as shown in Fig. 1(a). In the field sweep at 16 mK, a round peak occurs at 63 mT, moving to lower fields as the temperature is raised, as shown in Fig. 1(b). The peak vanishes completely between 85 mK and 100 mK. Most significantly, a second peak appears at 0.59 T (the internal field $H_{int} \simeq 0.53$ T), as shown in Fig. 1(c) [35]. This smaller, broader peak also moves to lower fields as the temperature is raised, becoming a very weak shoulder at 50 mK and disappearing before the temperature reaches 70 mK. This peak is distinct from the weak anomaly observed by Legl *et al.* [15] in the derivative of magnetization, dM/dH, at a higher field of 1.9 T ($H_{int} \simeq 1.3$ T) at 70 mK. It is very likely that that shoulder-like feature corresponds to the similar one in our data at about 1.2 T ($H_{int} \simeq 1.0$ T), shown in Fig. 1(d) [35].

The positions of the χ' peaks are summarized in Fig. 2, which suggests the existence of two new phases—phase I, bounded at about 140 mK in zero field and at about 70 mT in the limit of zero temperature, and phase II, bounded at about 0.60 T in the same limit. As shown in the inset, the upper boundary of phase II exists up to about 40 mK but, unlike that of phase I, it gradually disappears at higher temperatures. This absence of a clear phase boundary to the high-temperature disordered phase is reminiscent of a classical kagome ice [28].

The field dependence of χ' at 16 mK, with two peaks, indicates the presence of a weak magnetization plateau in phase II, between 63 mT and 0.59 T. This finding lends support to the quantum kagome-ice state predicted by the single-tetrahedron four-spin model and, by implication, to the underlying proposal [24] that the low-field ground state of $Tb_2Ti_2O_7$ is a quantum spin ice. The temperature at which the second peak becomes evident, 40 mK, is consistent with this prediction, strongly suggesting that the energy scale of the model is correct. The two critical fields, however, are higher than predicted, by a factor of about three and seven, respectively [35], suggesting that the field dependence of the energy level of the three-in one-out state may be strongly affected by many-tetrahedron effects, which are absent from the model.

Figures 3(a) and 3(b) show the real and imaginary parts, χ' and χ'', of the susceptibility near the χ' peak at zero field and at equilibrium, for three frequencies. At 0.21 Hz, a round peak appears in χ' at about 140 mK. With increasing frequency, the χ' peak becomes wider and moves to slightly higher temperatures. A peak also appears in χ'' about 30 mK below the χ' peak. Previous susceptibility measurements [10] have observed a similar frequency dependence, but with a broad peak at 16 Hz

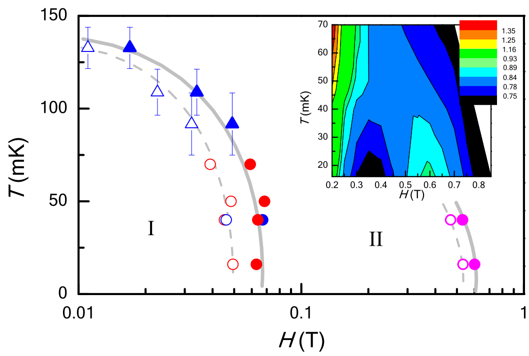

FIG. 2. (color online). H-T phase diagram determined from the χ' peak positions. Triangles are from the temperature sweeps, with peak positions in downward and upward sweeps averaged. Circles are from field sweeps. Red and magenta circles: from the data shown in Figs. 1(b) and(c); blue circle: from 0.21 Hz data, for which the ac amplitude and the field-sweep rate were 0.94 mT and 0.51 mT/min. Open symbols are the same data plotted against H_{int}. Lines are guides to the eye. Inset: contour plot of χ' in the H-T plane in and near phase II, constructed from field and temperature sweeps at 9.6 Hz.

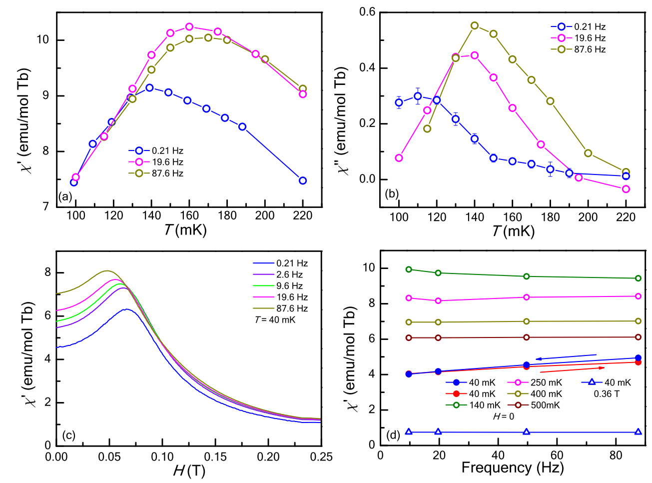

FIG. 3. (color online). Equilibrium χ' (a) and χ'' (b) near the χ' peak in zero field. (c) χ' at 40 mK as a function of magnetic field at various frequencies. The field was swept upward at 4.2 mT/min. For all panels, the ac-field amplitude H_{ac} was 0.94 mT. Thus, in panels (a) and (b), the 87.6 Hz data near 100 mK were taken in a slightly nonlinear regime. Similarly, the 87.6 Hz data in panel (c) were from a slightly nonlinear regime, at least at $H=0$ (see the Supplemental Material [33]). (d) χ' at $H=0$ and 0.36 T as a function of frequency at various temperatures. H_{ac} was 0.20 mT. For the 40 mK data at $H=0$, arrows indicate the directions of frequency steps, showing a weak hysteresis. Hysteresis is absent from all the other data. See the Supplemental Material [33] for the imaginary part of the data shown in panel (c).

appearing at about 250 mK, clearly higher than 160 mK at 19.6 Hz for our sample. Measurements by other groups [11, 14] have also found a similar frequency dependence, with peaks in χ' and χ'' occurring at temperatures closer to ours, for an ac field applied along [001] or [110].

The shift of a χ' peak to a higher temperature caused by increasing the frequency, observed in these and our measurements, is reminiscent of a spin-glass transition [36], as is the appearance of a sharper peak in χ''. Moreover, we find that the χ'-peak shift per decade frequency is $\Delta T_p/(T_p \log f) = 0.075$, where T_p is the peak temperature and f the frequency, consistent with 0.06–0.08 from more extensive measurements [14] and similar to that of a spin-glass transition in an insulator [36]. However, the downward shift of a χ' peak with increasing field (Fig. 1(a)) is not found in a canonical spin glass, where application of a field instead moves the peak slightly upward in temperature [36].

The peak position in field sweeps also depends on the frequency, moving to lower fields with increasing frequency, as shown in Fig. 3(c). Therefore, the boundary of phase I drawn in Fig. 2 is frequency-dependent. Moreover, χ' at zero field increases linearly with increasing frequency and exhibits slight hysteresis, as shown in Fig. 3(d). This frequency dependence is much weaker at and above 140 mK, outside phase I, and is absent at 0.36 T, well into phase II.

Although its mechanism is not understood, this peculiar frequency dependence of χ' allows us to accurately measure the relaxation time of spins by stepping the frequency, which—unlike temperature—can be changed nearly instantaneously. Figure 4(a) shows the total magnitude, $|\chi|$, of the susceptibility at 40 mK at zero field, as the frequency was changed stepwise between 9.6 Hz and 389.6 Hz, first upward then downward. $|\chi|$, instead of χ' alone, is fitted to a stretched exponential $\exp[-(t/\tau)^\alpha]$ to extract the relaxation time τ, because both χ' and χ'' evolve with time after a frequency step. The stretching exponent α ranges from 0.94 to 1.10, indicating that the relaxation is nearly exponential. The relaxation time is a strong function of frequency at this temperature, as shown in Fig. 4(b). It also depends strongly on temperature, as Fig. 4(c) shows, with an abrupt rise within a narrow temperature interval between 120 mK and 130 mK, where χ'' rises sharply (see Fig. 3(b)). The relaxation time measured at 0.21 Hz up to 120 mK can be expressed by an empirical formula for spin glasses [37], $1/\tau \sim \exp[-a(T_p/T)]$ with $a = 0.41$ and $T_p = 140$ mK, as shown in Fig. 4(d). Note that even at 140 mK, the relaxation rate, $1/\tau$, is as small as $7.1 \times 10^{-3}\,\mathrm{s}^{-1}$, two orders of magnitude smaller than even our lowest measuring frequency, indicating that much of the susceptibility we have measured is in the adiabatic limit, not the isothermal limit.

A similar temperature dependence has been found in a spin glass [38, 39]. Unlike in our case, however, the relaxation is logarithmic in time, as predicted by the droplet scaling theory [40], not nearly exponential. To

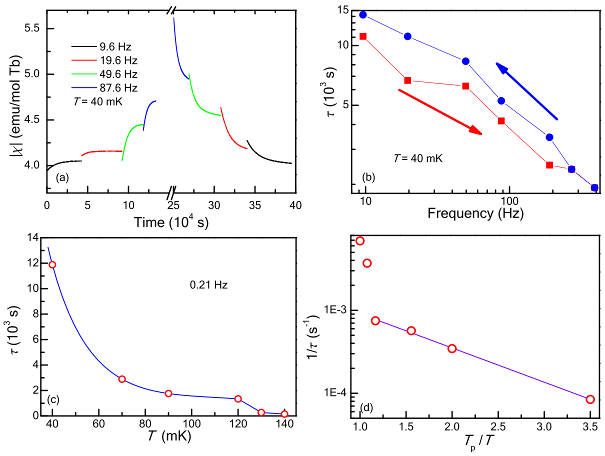

FIG. 4. (color online). (a) $|\chi|$ as a function of time at 40 mK in zero field. Before $t=0$, the ac frequency was held at 2.6 Hz for 12 hours until equilibrium was reached. Thereafter, the frequency was changed stepwise, each time after new equilibrium was reached. For clarity, relaxation curves at 189.6 Hz, 269.6 Hz, and 389.6 Hz—between the two 87.6 Hz curves—are not shown. (b) Relaxation time τ as a function of frequency, extracted from the data. Arrows indicate the frequency-step sequence. (c) τ *vs* temperature. At each temperature, the frequency was first held at 389.6 Hz until equilibrium was reached, then stepped down to 0.21 Hz, the frequency at which the measurements were made. (d) $1/\tau$ *vs* T_p/T, where $T_p = 140$ mK. For all the panels, $H_{ac} = 0.20$ mT.

our knowledge, relaxation rates much smaller than measuring frequencies have not been observed in a spin glass.

In summary, we have constructed, from ac magnetic susceptibility, a low-temperature magnetic phase diagram of $Tb_2Ti_2O_7$ in low magnetic fields applied along [111], uncovering two phases. The field dependence of the susceptibility at 16 mK and 40 mK indicates the presence of a weak magnetization plateau in support of theory [24, 25], suggesting that phase II is a quantum kagome ice. In view of the underlying proposal of the theory, phase I is likely to be a quantum spin ice. The frequency dependence of the susceptibility-peak position at zero field is similar to that of a spin glass, as is the temperature dependence of the relaxation time. But the field dependence of the peak position and the time dependence of the relaxation, as well as the frequency and amplitude dependence of χ' at 40 mK, suggest that phase I is not a spin glass.

In addition to our work, three very recent studies have investigated $Tb_2Ti_2O_7$ in magnetic fields applied along [111], also motivated by the prediction on the low-field ground state by the theory. Lhotel *et al.* [14] measured the magnetization up to 8 T and ac susceptibilities at zero field, and found no evidence for a magnetization plateau. However, the lowest temperature of the experiment was 80 mK, insufficient to detect the weak plateau indicated by our susceptibility result. Legl *et al.* [15] also measured the magnetization, to a lower temperature of 43 mK, yet finding no evidence for a plateau. In particular, the derivative dM/dH exhibits no anomaly that corresponds to the second χ' peak we have observed at and below 40 mK. Our results shown in Fig. 1(c) suggest, however, that 43 mK may not be cold enough to clearly detect such an anomaly. Moreover, the field-sweep rate employed by Legl *et al.* was four times faster than the rate we have found at 40 mK to completely wipe out the peak (see the Supplemental Material [33]). The low-field low-temperature phase diagram proposed by these authors also differs substantially from ours. However, at least part of the discrepancy may come from the much faster temperature-sweep rate—5 mK/min as opposed to our 0.6 mK/min—used by Legl *et al.*. Baker *et al.* [16] measured μSR to 25 mK and ac susceptibility to 68 mK. They have observed anomalies in the μSR relaxation time at 15 mT and $\sim$60 mT, at and below 50 mK. The susceptibility χ' at 68 mK and 100 mK, measured at 50 Hz and 500 Hz, is similar to ours but shows a broad peak at about 15 mT, lower than the positions of the peak we have found at 9.6 Hz and 87.6 Hz at similar temperatures (Fig. 1(b)). The temperature and field ranges of the experiment were not sufficient to observe the second peak, the key signature of the weak magnetization plateau.

We thank C. P. Aoyama for making SQUID-magnetometer measurements for calibration and P. J. Baker and H. D. Zhou for helpful discussions. The experiment was performed at the NHMFL High B/T Facility, which is supported by NSF Grant DMR 0654118 and by the State of Florida. Q. J. L. and X. F. S. acknowledge supports from the National Natural Science Foundation of China, the National Basic Research Program of China (Grant Nos. 2009CB929502 and 2011CBA00111), and the Fundamental Research Funds for the Central Universities (Program No. WK2340000035).

* yin@phys.ufl.edu
† xfsun@ustc.edu.cn

[1] For a review, see J. S. Gardner, M. J. P. Gingras, and J. E. Greedan, Rev. Mod. Phys. **82**, 53 (2010).
[2] A. P. Ramirez, A. Hayashi, R. J. Cava, R. Siddharthan, and B. S. Shastry, Nature (London) **399**, 333 (1999).
[3] D. J. P. Morris, D. A. Tennant, S. A. Grigera, B. Klemke, C. Castelnovo, R. Moessner, C. Czternasty, M. Meissner, K. C. Rule, J. U. Hoffmann, K. Kiefer, S. Gerischer, D. Slobinsky, and R. S. Perry, Science **326**, 411 (2009).
[4] S. T. Bramwell and M. J. P. Gingras, Science **294**, 1495 (2001).
[5] M. J. Harris, S. T. Bramwell, D. F. McMorrow, T. Zeiske, and K. W. Godfrey, Phys. Rev. Lett. **79**, 2554 (1997).
[6] A. Yaouanc, P. Dalmas de Réotier, V. Glazkov, C. Marin, P. Bonville, J. A. Hodges, P. C. M. Gubbens, S. Sakarya, and C. Baines, Phys. Rev. Lett. **95**, 047203 (2005).
[7] J. Lago, T. Lancaster, S. J. Blundell, S. T. Bramwell, F.

L. Pratt, M. Shirai, and C. Baines, J. Phys.: Condens. Matter **17**, 979 (2005).

[8] J. S. Gardner, S. R. Dunsiger, B. D. Gaulin, M. J. P. Gingras, J. E. Greedan, R. F. Kiefl, M. D. Lumsden, W. A. MacFarlane, N. P. Raju, J. E. Sonier, I. Swainson, and Z. Tun, Phys. Rev. Lett. **82**, 1012 (1999).

[9] G. Luo, S. T. Hess, and L. R. Corruccini, Phys. Lett. A **291**, 306 (2001).

[10] J. S. Gardner, A. Keren, G. Ehlers, C. Stock, E. Segal, J. M. Roper, B. Fåk, M. B. Stone, P. R. Hammar, D. H. Reich, and B. D. Gaulin, Phys. Rev. B **68**, 180401 (2003).

[11] N. Hamaguchi, T. Matsushita, N. Wada, Y. Yasui, and M. Sato, Phys. Rev. B **69**, 132413 (2004).

[12] A. Yaouanc, P. Dalmas de Réotier, Y. Chapuis, C. Marin, S. Vanishri, D. Aoki, B. Fåk, L. P. Regnault, C. Buisson, A. Amato, C. Baines, and A. D. Hillier, Phys. Rev. B **84**, 184403 (2011).

[13] H. Takatsu, H. Kadowaki, T. J. Sato, J. W. Lynn, Y. Tabata, T. Yamazaki, and K. Matsuhira, J. Phys.: Condens. Matter **24**, 052201 (2012).

[14] E. Lhotel, C. Paulsen, P. Dalmas de Réotier, A. Yaouanc, C. Marin, and S. Vanishri, Phys. Rev. B **86**, 020410(R) (2012).

[15] S. Legl, C. Krey, S. R. Dunsinger, H. A. Dabkowska, J. A. Rodriguez, G. M. Luke, and C. Pfeiderer, Phys. Rev. Lett. **109**, 047201 (2012).

[16] P. J. Baker, M. J. Matthews, S. R. Giblin, P. Schiffer, C. Baines, and D. Prabhakaran, Phys. Rev. B **86**, 094424 (2012).

[17] T. Fennell, M. Kenzelmann, B. Roessli, M. K. Haas, and R. J. Cava, Phys. Rev. Lett. **109**, 017201 (2012).

[18] J. A. Hodges, P. Bonville, A. Forget, A. Yaouanc, P. Dalmas de Réotier, G. André, M. Rams, K. Królas, C. Ritter, P. C. M. Gubbens, C. T. Kaiser, P. J. C. King, and C. Baines, Phys. Rev. Lett. **88**, 077204 (2002).

[19] K. A. Ross, J. P. C. Ruff, C. P. Adams, J. S. Gardner, H. A. Dabkowska, Y. Qiu, J. R. D. Copley, and B. D. Gaulin, Phys. Rev. Lett. **103**, 227202 (2009).

[20] K. A. Ross, L. R. Yaraskavitch, M. Laver, J. S. Gardner, J. A. Quilliam, S. Meng, J. B. Kycia, D. K. Singh, Th. Proffen, H. A. Dabkowska, and B. D. Gaulin, Phys. Rev. B **84**, 174442 (2011).

[21] L.-J. Chang, S. Onoda, Y. Su, Y.-J. Kao, K.-D. Tsuei, Y. Yasui, K. Kakurai, and M. R. Lees, Nature Comm. **3**, 392 (2012).

[22] M. J. P. Gingras, B. C. den Hertog, M. Faucher, J. S. Gardner, S. R. Dunsiger, L. J. Chang, B. D. Gaulin, N. P. Raju, and J. E. Greedan, Phys. Rev. B **62**, 6496 (2000).

[23] I. Mirebeau, P. Bonville, and M. Hennion, Phys. Rev. B **76**, 184436 (2007).

[24] H. R. Molavian, M. J. P. Gingras, and B. Canals, Phys. Rev. Lett. **98**, 157204 (2007).

[25] H. R. Molavian and M. J. P. Gingras, J. Phys.: Condens. Matter **21**, 172201 (2009).

[26] R. Moessner, O. Tchernyshyov, and S. L. Sondhi, J. Stat. Phys. **116**, 755 (2004).

[27] T. Sakakibara, T. Tayama, Z. Hiroi, K. Matsuhira, and S. Takagi, Phys. Rev. Lett. **90**, 207205 (2003).

[28] Y. Tabata, H. Kadowaki, K. Matsuhira, Z. Hiroi, N. Aso, E. Ressouche, and B. Fåk, Phys. Rev. Lett. **97**, 257205 (2006).

[29] J. S. Gardner, B. D. Gaulin, and D. McK. Paul, J. Cryst. Growth **191**, 740 (1998).

[30] L. Yin, J. S. Xia, V. S. Zapf, N. S. Sullivan and A. Paduan-Filho, Phys. Rev. Lett. **101**, 187205 (2008).

[31] L. Yin, J. S. Xia, V. S. Zapf, N. S. Sullivan, and A. Paduan-Filho, J. Low Temp. Phys. **158**, 710 (2010).

[32] R. Yu, L. Yin, N. S. Sullivan, J. S. Xia, C. Huan, A. Paduan-Filho, N. F. Oliveira, S. Haas, A. Steppke, C. F. Miclea, F. Weickert, R. Movshovich, E. D. Mun, V. S. Zapf, and T. Roscilde, Nature **489**, 379 (2012).

[33] See Supplemental Material at http://link.aps.org/supplemental/.... for the effect of the slow spin relaxation on data taken during temperature sweeps and field sweeps, temperature-sweep data at and above 0.1 T, an ac-field amplitude dependence of the susceptibility in phase I, and the imaginary parts of the data shown in Figs. 1 and 3(c).

[34] All χ' and χ'' in this Letter and the Supplemental Material have been corrected for the demagnetizing effect. See, for instance, C. Dekker, A. F. M. Arts, H. W. de Wijn, A. J. van Duyneveldt, and J. A. Mydosh, Phys. Rev. B **40**, 11243 (1989).

[35] Using an average demagnetization factor for our sample, 0.23, we estimate the internal fields, H_{int}, of the three anomalies marked in Fig. 1(d) to be 48 mT, 0.53 T, and 1.0 T. This should be compared with the applied fields, 63 mT, 0.59 T, and 1.2 T.

[36] J. A. Mydosh, *Spin Glasses: An Experimental Introduction* (Taylor and Francis, London, 1993).

[37] R. Hoogerbeets, W. L. Luo, and R. Orbach, Phys. Rev. Lett. **55**, 111 (1985).

[38] P. Svedlindh, K. Gunnarsson, J-O. Andersson, H. Aruga Katori, and A. Ito, Phys. Rev. B **46**, 13867 (1992).

[39] L. Lundgren, P. Svedlihdh and O. Beckman, J. Mag. Mag. Mat. **31-34**, 1349 (1983).

[40] D. S. Fisher and D. A. Huse, Phys. Rev. B **38**, 373 (1988).